Journal of Power Sources 185 (2008) 776–783

Contents lists available at ScienceDirect

Journal of Power Sources

journal homepage: www.elsevier.com/locate/jpowsour

Oxidation of methanol on perovskite-type $La_{2-x}Sr_xNiO_4$ ($0 \le x \le 1$) film electrodes modified by dispersed nickel in 1 M KOH

R.N. Singh[a,*], A. Singh[a], D. Mishra[a], Anindita[a], P. Chartier[b]

[a] Department of Chemistry, Faculty of Science, Banaras Hindu University, Varanasi 221 005, India
[b] Laboratoire d'Electrochimie et Chimie Physique du Corps Solide, Institut de Chimie LC3-UMR7177 CNRS/ULP, Universite Louis Pasteur, 67000, Strasbourg, France

ARTICLE INFO

Article history:
Received 24 April 2008
Received in revised form 16 June 2008
Accepted 4 July 2008
Available online 5 August 2008

Keywords:
Electro-oxidation
Direct methanol fuel cell
Perovskite electrode
Current density
Nickel particles

ABSTRACT

Finely-dispersed nickel particles are electrodeposited on high surface-area perovskite-type $La_{2-x}Sr_xNiO_4$ ($0 \le x \le 1$) electrodes for possible use in a direct methanol fuel cell (DMFC). The study is conducted by cyclic voltammetry, chronoamperometry, impedance spectroscopy and anodic Tafel polarization techniques. The results show that the apparent electrocatalytic activities of the modified oxide electrodes are much higher than those of unmodified electrodes under similar experimental conditions; the observed activity is the greatest with the modified $La_{1.5}Sr_{0.5}NiO_4$ electrode. At 0.550 V (vs. Hg|HgO) in 1 M KOH + 1 M CH_3OH at 25 °C, the latter electrode delivers a current density of over 200 mA cm^{-2}, whereas other electrodes of the series produce relatively low values (65–117 mA cm^{-2}). To our knowledge, such high methanol oxidation current densities have not been reported on any other non-platinum electrode in alkaline solution. Further, the modified electrodes are not poisoned by methanol oxidation intermediates/products.

1. Introduction

Direct methanol fuel cells (DMFCs) are promising electrochemical energy converters for a variety of applications due to their simplicity, low pollution and high efficiency [1–3]. Nevertheless, commercialization of DMFCs suffers from two major problems, namely, a high overpotential (η) for the methanol oxidation reaction (MOR) [4,5] and methanol crossover from the anode to the cathode [6,7]. The latter problem can be minimized by using a low methanol concentration and employing a modified proton exchange membrane (PEM) [8]. In order to improve the reaction kinetics and lower the overpotential, considerable efforts have recently been made towards developing new electrodes with greatly enhanced electrocatalytic activities [9–30]. Most of these investigations have focused on Pt-based or Pt-Ru bimetallic systems mainly in acid electrolytes. Although Pt is a very efficient electrocatalyst for the MOR, it suffers loss in activity with time due to accumulation of surface poisoning intermediates such as CO formed during the oxidation reaction [5]. Moreover, noble metals are expensive and not readily available. There is naturally a serious demand to develop inexpensive and active electrode materials from non-noble metals for use as anodes in alkaline DMFCs. An alkaline electrolyte is considered superior to an acid one in respect of both, kinetics and material stability. A much wider range of materials, particularly pure as well as mixed oxides, are stable in alkaline solutions and can be used either as anodes or support materials for the dispersion of noble and other metals.

Oxides of V, Fe, Ni, In, Sn, La, and Pb [31] as anode materials have not shown any practical activity for methanol oxidation. By contrasts graphite supported perovskite-modified Pt electrodes exhibit much higher electrocatalytic activities, compared with smooth Pt or graphite supported-Pt electrodes, towards MOR in 1 M NaOH at 25 °C [32]. Recently, Raghuveer and Vishwanathan [33] investigated the electro-oxidation of methanol on bulk and nanocrystalline $La_{1.8}Sr_{0.2}CuO_4$ in 1 M KOH + 1 M CH_3OH and observed currents of 1.9 and 5.2 mA cm^{-2} at 0.6 V (vs. Ag|AgCl (scan rate = 25 mV s^{-1}), respectively. Raghuveer et al. [34] obtained 0.38, 1.47 and 1.84 mA cm^{-2} at E = 0.60 V (vs. Hg|HgO) on $La_{1.8}Sr_{0.2}CuO_4$, $La_{1.6}Sr_{0.4}CuO_4$ and $La_{1.9}Sr_{0.1}Cu_{0.9}Sb_{0.1}O_4$ in 3 M KOH + 2 M CH_3OH. Similar studies carried out by Yu et al. [35] gave 18.8 and 7.7 mA cm^{-2} on $La_{0.75}Sr_{0.25}CuO_{3-\delta}$ and $La_{0.75}Sr_{0.25}CoO_{3-\delta}$ at E = 0.60 V (vs. Ag|AgCl) in 1 M NaOH + 1 M CH_3OH (scan rate = 20 mV s^{-1}).

Recently, Deshpande et al. [36] prepared a variety of ABO_3 and A_2BO_4 perovskite oxides (A = Sr, Ce, La and B = Co, Fe, Ni, Pt, Ru) by means of aqueous solution combustion synthesis and then measured their catalytic performance for methanol electro-oxidation by a rapid screening approach (NuVant System). They found that

* Corresponding author. Tel.: +91 542 6701596; fax: +91 542 2368127.
E-mail addresses: rnsbhu@rediffmail.com (R.N. Singh), mitbhu@gmail.com (A. Singh), diya_chem@yahoo.co.in (D. Mishra), ani3684@rediffmail.com (Anindita), pierre-chartier2@orange.fr (P. Chartier).

0378-7753/$ – see front matter © 2008 Elsevier B.V. All rights reserved.
doi:10.1016/j.jpowsour.2008.07.078

the performance of Sr-based perovskites was comparable with that of the standard Pt-Ru catalyst. Using a similar method, Lan and Mukasyan [37] synthesized a series of perovskites (ABO_3; A = Ba, Ca, Sr, La; B = Fe, Ru) and carried out their electrochemical characterization for methanol oxidation under conditions similar to those for DMFCs. The study demonstrated that the perovskites containing ruthenium at the B-site were promising candidates for the development of effective catalysts.

Very recently [38], we have prepared perovskite-type $La_{2-x}Sr_xNiO_4$ ($0 \le x \le 1$) oxides by a modified citric acid sol–gel route and used them as anodes for the electrocatalysis of methanol oxidation in 1 M KOH. These new electrodes have produced much higher current densities than those already reported for other perovskite oxides [33–35] under alkaline conditions, namely, 23.6, 47.3, 43.2 and 50.9 mA cm^{-2} for electrodes with $x = 0$, $x = 0.25$, $x = 0.5$ and $x = 1.0$, respectively, at 10 mV s^{-1} and $E = 0.60$ V (vs. Hg|HgO) in 1 M KOH + 1 M CH_3OH (25 °C). More importantly, these complex oxide anodes have not shown any surface poisoning during methanol oxidation by the intermediate products. To improve their electrocatalytic activities, the electrodes have been modified by dispersed nickel and have been investigated for their electrocatalytic properties towards the MOR in 1 M KOH. The results of this investigation are described here.

2. Experimental

2.1. Electrode synthesis

2.1.1. Materials

Methanol (Merck, GR), potassium hydroxide (Merck, GR), $Ni(NO_3)_2{\cdot}6H_2O$ (Merck, 97%), $La(NO_3)_3{\cdot}6H_2O$ (Merck, 99%, GR), $Sr(NO_3)_2$ (CDH, 99.5%, AR), $(CH_3COO)_2Ni{\cdot}4H_2O$ (Reidel, 99.5%, AR), L-ascorbic acid (s.d.fine., AR), boric acid (Merck, 99.5%) and nickel foil (0.25 mm thick, Aldrich 99.98%) were used as-received. Redistilled water was used for preparation and dilution of all the solutions.

2.1.2. Preparation of $La_{2-x}Sr_xNiO_4$ electrodes

Perovskite oxides, namely La_2NiO_4, $La_{1.75}Sr_{0.25}NiO_4$, $La_{1.5}Sr_{0.5}NiO_4$ and $LaSrNiO_4$ were synthesized by a modified citric acid sol–gel precursor method [39,40]. In this method, nitrates of the constituent metals (La, Sr, Ni) of the oxides were dissolved, as per stoichiometry, in 100 ml of distilled water (total metal ion concentration = 0.23–0.26 M) and to this solution a slightly excess quantity of citric acid (CA = 0.231–0.2605 M), 2.0 ml of ethylene glycol (E. Merck, Germany) and finally two drops of concentrated HNO_3 were added. Vigorous stirring was carried out while adding these ingredients. A gel was soon formed which was heated slowly to effect decomposition. The resulting substance was fired at 100 °C to ash which was ground with an Agate pestle and mortar and calcined at 600 °C for 6 h to obtain the desired products. The oxides, thus obtained, have a tetragonal primitive crystal structure with a crystallite size of 9–12 nm [40].

The electrodes of the oxides (i.e. Ni/$La_{2-x}Sr_xNiO_4$) were obtained by painting a slurry containing the oxide powder and glycerol on to a pretreated nickel plate followed by sintering at 380 °C for 1.5 h. Pretreatment of the support and electrical contact with the oxide films were made as described previously [41]. The oxide loadings were 4–5 mg cm^{-2}.

2.1.3. Preparation of Ni-modified $La_{2-x}Sr_xNiO_4$ electrodes

Nickel was electrodeposited on $La_{2-x}Sr_xNiO_4$ electrodes from an acetate bath at a constant pH of 5.2 as reported elsewhere [42]. The composition of the electrolytic bath was 0.28 M nickel acetate + 0.4043 M boric acid + 10 mg ascorbic acid + 3 drops acetic acid. Electrodeposition was carried out at 25 °C in a conventional three-electrode, single-compartment, Pyrex glass cell at a constant current density of 20 mA cm^{-2} for 300 s. The auxiliary and reference electrodes were Pt-foil and Hg|HgO, respectively. After deposition, the complex oxide electrode (i.e., Ni/$La_{2-x}Sr_xNiO_4$/Ni) was removed from the cell, washed with distilled water, dried in air, and then used for the study.

2.2. Electrocatalyst characterization

2.2.1. Physicochemical

Nickel deposited on $La_{2-x}Sr_xNiO_4$ was examined by a SEM–EBSD integrated system (Hitachi, S3400N). The mass of electrodeposited nickel on each oxide film was determined by analyzing the electrolytic bath solution before and after Ni deposition by means of an atomic absorption spectrophotometer (AAS – PerkinElmer – 2380). The particle size of the powders used for preparation of the oxide electrode was measured with a particle size and shape analyzer (ANKERSMID, Holland).

2.2.2. Electrochemical

A conventional three-electrode, single-compartment, Pyrex glass cell, fitted with a pure Pt-foil (~8 cm^2) counter electrode and a Hg|HgO|1 M KOH reference electrode, was employed for electrochemical investigations. Cyclic voltammetry (CV), electrochemical impedance spectroscopy (EIS) and Tafel polarization studies were conducted with an electrochemical impedance system (PARC, USA) attached with a potentiostat/galvanostat (Model 273 A), a lock-in-amplifier (5210) and a computer (COMPAQ P4). The CV of each electrocatalyst was investigated between 0 and 0.65 V (vs. Hg|HgO) in 1 M KOH with and without methanol at 25 °C. Before recording the final voltammogram, each electrode was cycled for five runs at a scanning rate (ν) of 50 mV s^{-1} in 1 M KOH. The anodic polarization curves (E vs. log j) were recorded using a run program with conditioning time = 200 s, conditioning potential = 0.35 V, initial delay = pass, $\nu = 0.2$ mV s^{-1}, initial potential = 0.35 V, and IR interruption = 10 s.

The EIS study of the electrodes was performed in 1 M KOH + 1 M CH_3OH with an ac voltage amplitude of 10 mV at a constant dc potential. The frequency range employed in the study was 0.1–25 × 10^3 Hz. The equivalent-circuit parameters were analyzed by the software, ZSimpWin.

All electrochemical experiments were performed in argon deoxygenated electrolytes at 25 °C. The potential values reported in the text are given against the Hg|HgO, 1 M KOH electrode.

3. Results and discussion

3.1. Morphology/particle size

Scanning electron micrograph (SEM) images of Ni as-deposited on La_2NiO_4, $La_{1.75}Sr_{0.25}NiO_4$, $La_{1.5}Sr_{0.5}NiO_4$ and $LaSrNiO_4$ show that the surface of each oxide consists of highly dispersed granules. The SEM images of two representative oxide catalysts, La_2NiO_4 and $La_{1.5}Sr_{0.5}NiO_4$ with and without Ni deposition, are presented in Fig. 1. The oxide surface unmodified with Ni seems to be somewhat less compact [38]. It is worth mentioning that all the oxide catalysts and procedures for obtaining their films were the same as reported elsewhere [38].

The quantity of Ni deposited on La_2NiO_4, $La_{1.75}Sr_{0.25}NiO_4$, $La_{1.5}Sr_{0.5}NiO_4$ $LaSrNiO_4$ films is 0.91, 2.79, 2.32, and 1.59 mg cm^{-2}, respectively.

Values of the mean particle size of powders of the oxide with $x = 0$, $x = 0.25$, $x = 0.5$ and $x = 1.0$ are 21.41, 19.38, 0.84 and 0.8 μm,

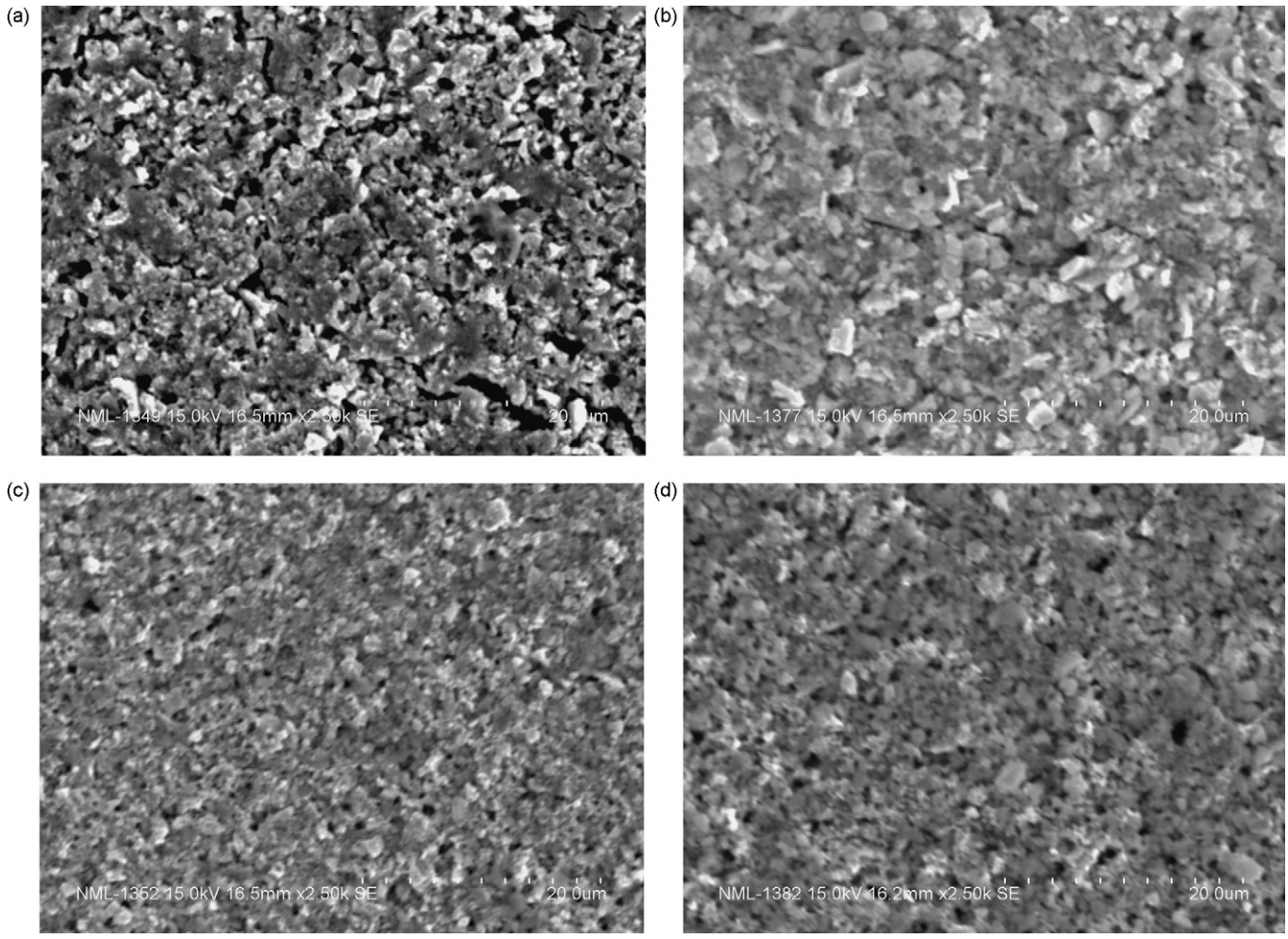

Fig. 1. Scanning electron micrographs of La_2NiO_4: (a) without and (b) with Ni deposition and of $La_{1.5}Sr_{0.5}NiO_4$: (c) without and (d) with Ni deposition.

respectively. A typical particle size histogram for $La_{1.5}Sr_{0.5}NiO_4$ is shown in Fig. 2.

3.2. Open-circuit potential (OCP) measurements

Prior to carrying out electrochemical investigations, each freshly prepared electrode was dipped into the electrolyte under an argon atmosphere and the potential of the electrode was monitored as a function of time (t) until it reached the steady open-circuit value (OCP). It is noted that in the case of electrodes modified with Ni, the electrode potential, in both 1 M KOH and 1 M KOH + 1 M CH_3OH, shifted gradually by about 300 mV in the noble direction with time and finally attained the OCP value in 20–25 min. In the case of unmodified electrodes, the OCP value is reached in 3 min, regardless of the immersion time and the type of electrolyte. Typical electrode potential shifts vs. time curves for the $La_{1.5}Sr_{0.5}NiO_4$ and modified $La_{1.5}Sr_{0.5}NiO_4$ electrodes are shown in Fig. 3. The shift of the electrode potential before reaching the OCP value with time can be ascribed to electrode surface modifications induced by the following reactions [43–44]:

$$Ni + 2OH^- \leftrightarrow Ni(OH)_2 + 2e^- \quad (1)$$

$$\alpha\text{-}Ni(OH)_2 \rightarrow \beta\text{-}Ni(OH)_2 \quad (2)$$

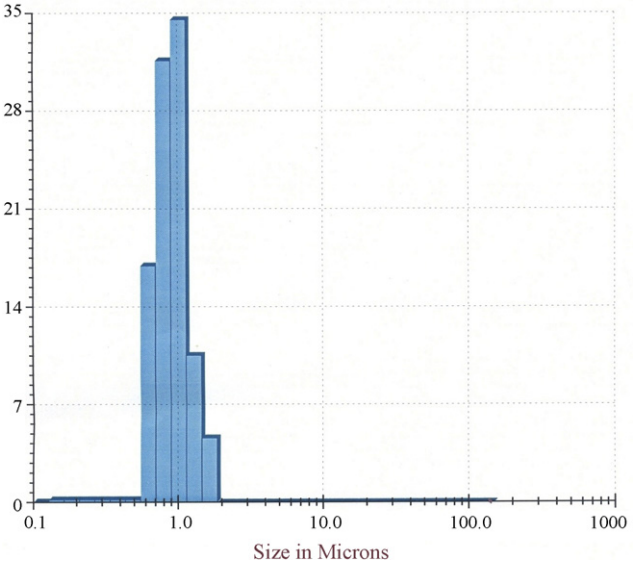

Fig. 2. Typical particle size histogram for $La_{1.5}Sr_{0.5}NiO_4$.

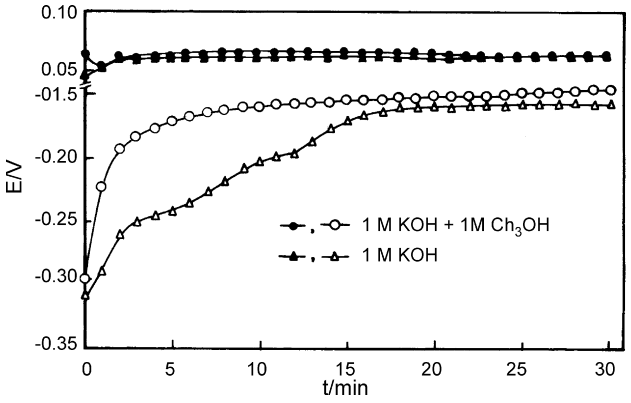

Fig. 3. Variation of open-circuit potential as function of immersion time for $La_{1.5}Sr_{0.5}NiO_4$ electrode without (●, ▲) and with (○, △) Ni deposition (25 °C).

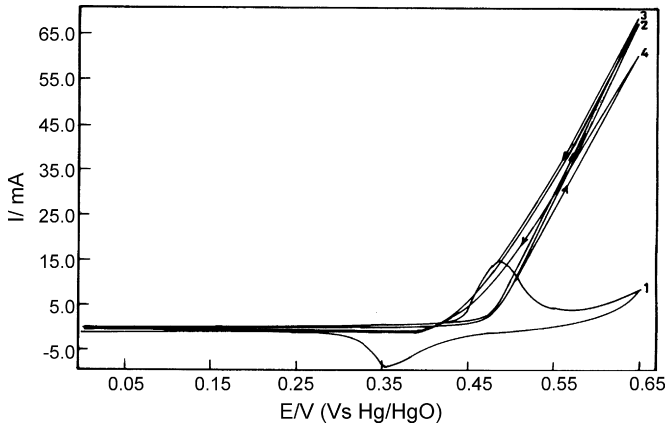

Fig. 4. Cyclic voltammograms for $La_{2-x}Sr_xNiO_4/NiO_y$ electrode in 1 M KOH with and without CH_3OH at 10 mV s^{-1}(25 °C). Curve, 1: $x = 0$ in 1 M KOH; curves, 2–4 correspond to $x = 0$, $x = 0.5$ and $x = 1$, respectively, in 1 M KOH + 1 M CH_3OH.

The E° value for reaction (1) is 0.55 V (vs. Hg/HgO/1 M NaOH). The phase transformation reaction (2) takes place in the potential region from 0.5 to 0.40 V (vs. Hg/HgO/1 M NaOH).

Values of the OCPs for the modified $La_{2-x}Sr_xNiO_4$ ($0 \le x \le 1$) electrodes, in 1 M KOH vis-a-vis in 1 M KOH + 1 M CH_3OH at 25 °C, are given in Table 1. The OCP measurements for the electrodes after polarization were also carried out and the steady OCP values, so obtained, are shown in Table 1. The electrode polarization was carried out by running cyclic voltammograms between 0 and 0.65 V at a scanning rate of 50 mV s^{-1} for five cycles. The data in Table 1 show that the OCP values for the electrodes after polarization are more positive than before polarization.

The higher OCP values for the $La_{2-x}Sr_xNiO_4/NiO_y$ electrodes after polarization can be attributed to the formation of a $Ni(OH)_2/NiO(OH)$ film [44]. Further, in 1 M KOH, the freshly prepared, modified oxide electrodes have significantly lower OCP values compared with those for the unmodified electrodes. The OCPs of fresh unmodified electrodes, in 1 M KOH (not shown in Table 1) are 0.004, 0.012, 0.040 and 0.003 V for La_2NiO_4, $La_{1.75}Sr_{0.25}NiO_4$, $La_{1.5}Sr_{0.5}NiO_4$ and $LaSrNiO_4$, respectively. The differences in OCP values can be attributed to the fact that prior to immersion in the electrolyte, the former electrode (modified) contains nickel in the reduced state on its surface, while the latter electrode (unmodified) contains the oxidized nickel species (Ni^{2+}/Ni^{3+}).

It is evident from the data Table 1 that the final value of the OCP for a $La_{2-x}Sr_xNiO_4/NiO_y$ electrode is the same in both 1 M KOH and 1 M KOH + 1 M CH_3OH solutions, but the electrode potential increases more slowly in 1 M KOH than in 1 M KOH + 1 M CH_3OH. This is possibly due to the adsorption of methanol molecules on the electrode surface. In fact, the adsorbed methanol molecules constitute an additional energy barrier, which increases the polarization of the anodic and cathodic processes.

Considering the OCP data and Ni–H_2O Pourbaix diagram, presence of the dispersed zero valent nickel on the $La_{2-x}Sr_xNiO_4$ surface seems to be unlikely and so the $Ni/La_{2-x}Sr_xNiO_4/Ni$ electrode system is represented by a better formalism, namely, $Ni/La_{2-x}Sr_xNiO_4/NiO_y$.

3.3. Cyclic voltammetry

Cyclic voltammograms for the $Ni/La_{2-x}Sr_xNiO_4$ ($0 \le x \le 1$)/NiO_y electrodes in 1 M KOH at 25 °C were determined at scanning rate of 10 mV s^{-1} in the potential range, 0–0.65 V. The voltammograms exhibit two redox peaks, an anodic ($E_{pa} = 496 \pm 13$ mV) and a corresponding cathodic ($E_{pc} = 363 \pm 4$ mV) peak, prior to the onset of the O_2 evolution reaction, revealing a pseudo-capacitance due to the Ni(III)/Ni(II) surface redox couple [41,44]. A typical voltammogram for the $Ni/La_2NiO_4/NiO_y$ electrode is shown in Fig. 4.

Voltammograms were also recorded for electrodes in 1 M KOH + 1 M CH_3OH. The curves obtained in each case are very similar (Fig. 4). For sake of clarity in representation, the voltammogram for the $Ni/La_{1.75}Sr_{0.25}NiO_4/NiO_y$ electrode is not shown in Fig. 4. In the presence of 1 M CH_3OH in 1 M KOH, it is seen that the area beneath the currents increases greatly, while the anodic and cathodic redox peaks of the Ni(III)/Ni(II) surface redox couple disappear. It is noted that these redox peaks do not appear even when voltammograms are recorded over scan rates of 1–100 mV s^{-1} in the case of the $Ni/La_{1.5}Sr_{0.5}NiO_4/NiO_y$ electrode. This indicates that methanol interacts strongly with the higher valence Ni(III) species and reduces them almost completely under anodic conditions so that little or no Ni(III) species is left for electrochemical reduction under cathodic conditions. In other words, the rate of reduction of Ni(III) species to Ni(II) species by interaction with methanol appears to occur more rapidly compared with the maximum applied scan rate (100 mV s^{-1}).

A comparison of voltammograms, determined in the presence and absence of methanol in the electrolyte, shows that the onset potential for methanol oxidation (0.45–0.46 V) is slightly higher than that for the electro-oxidation of Ni(II) to Ni(III) (0.422–0.426 V). This shows that the electro-oxidation of methanol

Table 1
OCP values for modified electrodes in 1 M KOH and 1 M KOH + 1 M CH_3OH under argon atmosphere at 25 °C

Electrodes	OCP (V)		
	1 M KOH (fresh)	1 M KOH + 1 M CH_3OH (fresh)	(after polarization)
$Ni/La_2NiO_4/NiO_y$	−0.142 ± 0.026	−0.129 ± 0.023	0.168
$Ni/La_{1.75}Sr_{0.25}NiO_4/NiO_y$	−0.174 ± 0.013	−0.165 ± 0.048	0.123
$Ni/La_{1.5}Sr_{0.5}NiO_4/NiO_y$	−0.194 ± 0.035	−0.150 ± 0.004	0.134
Ni/LaSrNiO4/NiO_y	−0.048 ± .028	−0.142 ± 0.026	0.166

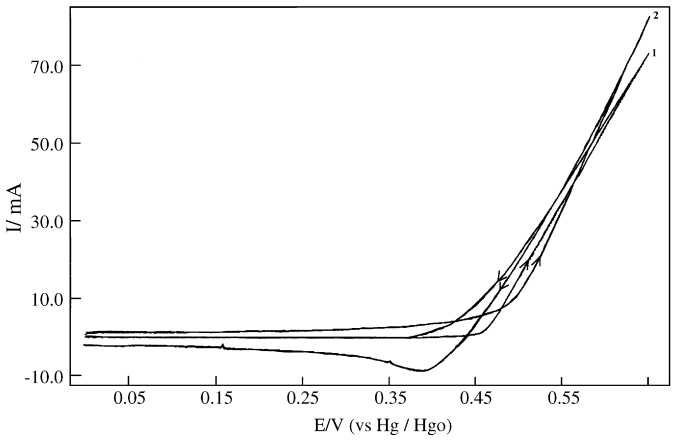

Fig. 5. Cyclic voltammograms for $La_{1.5}Sr_{0.5}NiO_4/NiO_y$ electrode at scan rates of 1 and 100 mV s^{-1} in 1 M KOH + 1 M CH_3OH at 25 °C.

occurs only on the Ni(III) surface. Further, a change in the scan rate (1–100 mV s^{-1}) does not influence the rate of oxidation of methanol. Two representative cyclic voltammograms, recorded at $\nu = 1$ and 100 mV s^{-1} in 1 M KOH + 1 M CH_3OH at 25 °C, are shown in Fig. 5. It is considered that electro-oxidation of CH_3OH proceeds through a mechanism that involves fast electrosorption of the CH_3OH molecule followed by fragmentation into intermediates on the surface sites towards the final oxidation products. The electrosorption of CH_3OH may be very fast and the surface becomes permanently saturated with adsorbed species in such a way that whatever the scan rate, and perhaps the concentration, the faradaic current remains the same.

3.4. Chronoamperometry

Chronoamperograms of electrodes recorded for nearly 5 h at a fixed anodic potential ($E = 0.5$) in 1 M KOH + 1 M CH_3OH are given in Fig. 6. With the passage of time, the current resulting from electro-oxidation of methanol initially increases, attains a maximum, decreases slightly, and remains constant. The nature of the current–time transient curves does not indicate any significant electrode poisoning by intermediates formed during the oxidation of CH_3OH in 1 M KOH. Further, the electrode, $Ni/La_{1.5}Sr_{0.5}NiO_4/NiO_y$ has the greatest apparent electrocatalytic activity whereas $Ni/LaSrNiO_4/NiO_y$ has the lowest.

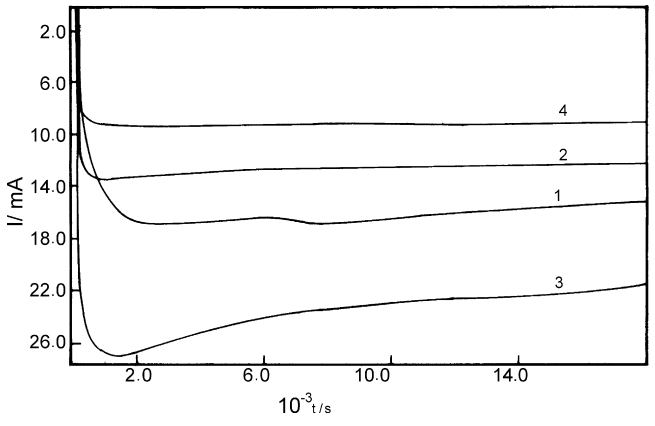

Fig. 6. Chronoamperograms for $La_{2-x}Sr_xNiO_4/NiO_y$ electrode at $E = 0.5$ V (vs. Hg|HgO) in 1 M KOH + 1 M CH_3OH (25 °C). Curves 1–4 correspond to $x = 0$, $x = 0.25$, $x = 0.5$ and $x = 1.0$, respectively.

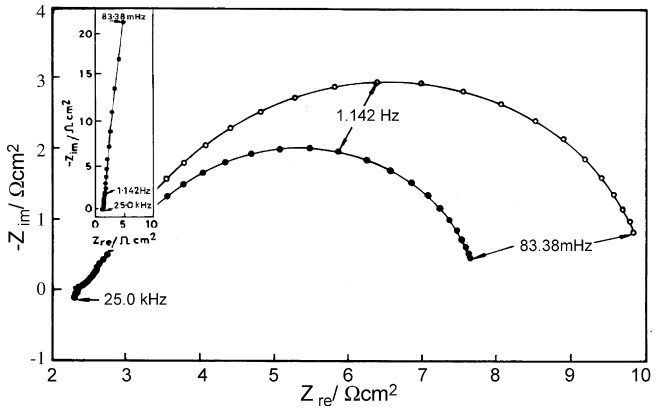

Fig. 7. Nyquist plots for $Ni/La_2NiO_4/NiO_y$ electrode at 25 °C in 1 M KOH + 1 M CH_3OH: E = (○) 0.475 and (●) 0.485 V; in 1 M KOH: E = 0.45V (inset).

On completion of the chronoamperometric experiments, $BaCl_2$ solution was added to the cell solution and showed the presence of carbonate as one of the products of the oxidation reaction. The electro-oxidation of methanol was carried out in a two-compartment (anodic and cathodic) cell. A gas sampler (~10 ml capacity) was connected to the anodic compartment to collect the CO gas. However, in a test of over 5 h at 0.50 V in 1 M KOH + 1 M CH_3OH at 25 °C, no CO formation was observed. This indicates that no gaseous product is formed. One cannot exclude, however, that beside CO_3^{2-}, non-gaseous products might form, such as formaldehyde or formate.

3.5. Electrochemical impedance spectroscopy (EIS)

In order to investigate the influence of the methanol electro-oxidation kinetics on impedance diagrams, impedance measurements at varying potentials (methanol oxidation region) were carried out on $Ni/La_{2-x}Sr_xNiO_4/NiO_y$ electrodes in argon-deoxygenated 1 M KOH + 1 M CH_3OH at 25 °C. Before recording each EI spectrum at a pre-selected dc potential, the working electrode was kept at this potential for 300 s to equilibrate. The features of the spectra obtained for each oxide anode are very similar.

The spectra for a Ni-modified La_2NiO_4 electrode at different potentials are shown in Fig. 7. There is a small potential-independent impedance in the high-frequency region (25 kHz to 20 Hz) that is followed by an intermediate, low-frequency arc. The diameter of this arc is observed to shrink with increasing E. This result indicates that the low frequency arc is associated with methanol electrooxidation [45–47] that is further confirmed by determining the Nyquist plot for the $Ni/La_2NiO_4/NiO_y$ electrode in 1 M KOH without CH_3OH. The latter curve (shown in the inset of Fig. 7) does not indicate the formation of a semicircle at the low frequency-end, instead, it shows capacitive behaviour. As already observed by de Silva et al. [48] for $IrO_2 + TiO_2$ ceramic film, a distorted small semi-circle is observed at high frequencies. This semi-circle was attributed to processes occurring in the more internal, porous part of the oxide layer.

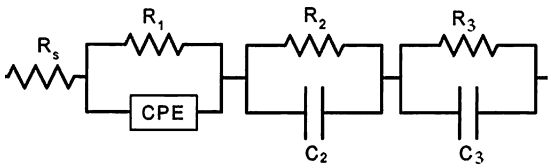

Fig. 8. Equivalent electrical circuit used to fit the experimental data of impedance spectra.

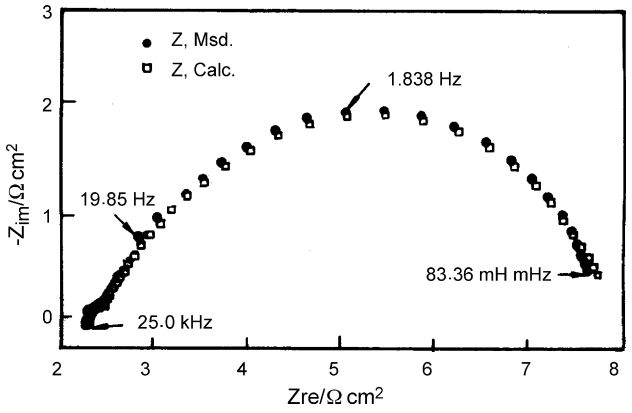

Fig. 9. Typical Nyquist plots (experimental + simulated) for Ni/La_2NiO_4/NiO_y electrode at E = 0.485 V in 1 M KOH + 1 M CH_3OH (25 °C).

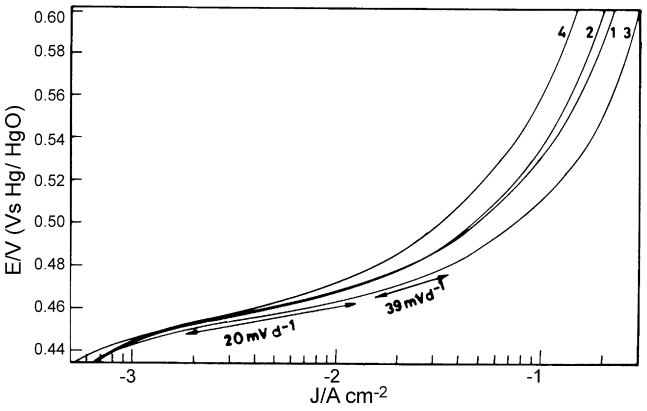

Fig. 10. Tafel plots for $La_{2-x}Sr_xNiO_4$/NiO_y electrodes (scan rate = 0.2 mV s^{-1}) in 1 M KOH + 1 M CH_3OH (25 °C). Curves 1–4 correspond to x = 0, x = 0.25, x = 0.5 and x = 1, respectively.

It is known [49–50] that when a granular oxide thin film comes into contact with a liquid electrolyte, the latter wets instantaneously the total surface of the powder. So, the developed surface can be reasonably considered to act like a planar surface. We, therefore, used a planar electrical equivalent-circuit composed of three capacitive/resistive elements in series so as to model the Ni/$La_{2-x}Sr_xNiO_4$/NiO_y/electrolyte system. The equivalent-circuit is shown in Fig. 8 and is similar to that earlier reported by Priyantha et al. [51].

The experimental data were analyzed by ZSimpWin Software using the above equivalent-circuit. Sub-circuits (R_1Q_1), (R_2C_2) and (R_3C_3) were used to account for contributions from the complex oxide ($La_{2-x}Sr_xNiO_4$) mass, $La_{2-x}Sr_xNiO_4$/NiO_y interface and electrode (NiO_y)|electrolyte interface, respectively. Symbols R_s, R_1, R_2 and R_3 are used to represent the electrolyte, bulk oxide ($La_{2-x}Sr_xNiO_4$), oxide|NiO_y interface, and charge-transfer resistance, respectively. Symbols Q_1, C_2 and C_3 represent constant phase element (CPE), capacitance of the oxide|NiO_y interface and the double-layer capacitance (C_{dl}) of the electrode|electrolyte interface, respectively. It is seen that the best fit of the experimental data is obtained only if an inductance, L, is included in the equivalent-circuit; the value of L is of the order of ~1 μH. The source of this inductive element is unclear, but wiring, measuring equipment components and heating sources may make possible contributions [48,52]. Based on the proposed circuit model, the EIS spectra obtained agree reasonably well with the experimental curves as shown for the Ni/La_2NiO_4/NiO_y electrode in Fig. 9. Estimates of the equivalent-circuit parameters are shown in Table 2, which also contains values of the electrode roughness factor (R_F). These values were estimated, as earlier [38], using the relation, R_F = (C_{dl} of test electrode)/(C_{dl} of a smooth oxide surface) = 60 μF cm^{-2}. The data in Table 2 show that the charge-transfer resistance (R_3) value at any electrode decreases, and hence the rate for methanol oxidation increases with increasing applied potential. Further, with the exception of the Ni/$LaSrNiO_4$/NiO_y electrode, all electrodes have almost similar values of the charge-transfer resistance for methanol oxidation. However, this would be clear from the study of Tafel polarization.

It is observed that when the surface of the electrodes, $La_{2-x}Sr_xNiO_4$ is modified by dispersed Ni, the double-layer capacitance, and hence the roughness factor of the electrode, is greatly enhanced. This can be judged from the C_{dl} values of 1.52, 1.02, 0.93 and 0.52 × 10^{-2} F cm^{-2} already observed for $La_{2-x}Sr_xNiO_4$ electrodes with x = 0, 0.25, 0.5 and 1.0, respectively (at E = 0.45 V vs. Hg|HgO in 1 M KOH + 1 M CH_3OH at 25 °C) [38].

3.6. Electrocatalytic activity

To test the electrocatalytic activity of oxide electrodes modified by dispersed nickel towards methanol oxidation in 1 M KOH + 1 M CH_3OH at 25 °C, ohmic (IR)-drop-compensated, steady-state, anodic polarization (E vs. log j) curves have been determined at a slow scanning rate of 0.2 mV s^{-1}, as shown in Fig. 10. The curves have not been corrected for background current (i.e., current produced in similar experiments carried out in 1 M KOH without containing methanol), because the values of the latter are less than 0.2 mA cm^{-2} in the potential region employed in the study (0.40–0.60 V). The nature of the plot for each modified oxide electrode, regardless of Sr content, is almost similar; the initial Tafel slopes (at low potentials) range between 20 and 40 mV $decade^{-1}$. Tafel slope values at the higher potentials are not well-defined, but appear to be greater than 80 mV $decade^{-1}$. The apparent electrocatalytic activities (j_a) of the modified oxide electrodes at two potentials, E = 0.55 and 0.60 V are given in Table 3.

Based on the apparent electrocatalytic activities (j_a) for methanol oxidation, the Ni/$La_{1.5}Sr_{0.5}NiO_4$/NiO_y electrode is found to be the most active (Table 3). Also, the true current density, j_t (=j_a/R_F), of this electrode appears to be the greatest for methanol oxidation. The electrode, Ni/$LaSrNiO_4$/NiO_y, has the lowest apparent, as well as the true, catalytic activity. This finding corroborates

Table 2
Values of equivalent-circuit parameters for Ni/$La_{2-x}Sr_xNiO_4$/NiO_y electrodes in 1 M KOH + 1 M CH_3OH at 25 °C, at E = 0.475 and 0.485 V (vs. Hg|HgO)

Electrode (x)	E (mV)	R_S (Ω cm^2)	R_1 (Ω cm^2)	$Q_1 \times 10^2$ (F s^{n-1} cm^{-2})	n_1	R_2 (Ω cm^2)	$C_2 \times 10^2$ (F cm^{-2})	R_3 (Ω cm^2)	$C_3 \times 10^2$ (F cm^{-2})	$R_F = 10^6$ C_3/60
0	475	2.3	5.4	4.58	0.68	0.11	6.12	2.67	5.76	1005 ± 70
0	485	2.3	3.8	4.58	0.68	0.10	7.83	1.77	6.46	
0.25	475	0.7	3.0	14.76	0.27	0.82	2.65	2.89	3.21	591 ± 56
0.25	485	0.7	2.3	10.59	0.32	0.66	3.07	1.79	3.88	
0.5	475	2.1	2.2	14.97	0.46	0.06	0.05	2.18	5.92	964 ± 24
0.5	485	2.0	1.7	32.47	0.28	0.25	5.30	1.87	5.64	
1.0	475	1.35	6.05	2.92	0.50	0.89	3.07	3.24	4.17	707 ± 12
1.0	485	1.42	4.32	2.89	0.51	0.93	2.133	2.21	4.31	

Table 3
Electrocatalytic activities of $La_{2-x}Sr_xNiO_4$ ($0 \le x \le 1$) electrodes, modified by dispersed Ni, in 1 M KOH + 1 M CH_3OH (25 °C)

Electrodes	Dispersed Ni mass (mg cm^{-2})	R_F	j (mA cm^{-2}) at E (V vs. Hg|HgO)			
			0.55		0.60	
			j_a	j_t	j_a	j_t
$Ni/La_2NiO_4/NiO_y$	0.91	~1005	117 ± 23	0.12	194 ± 30	0.19
$Ni/La_{1.75}Sr_{0.25}NiO_4/NiO_y$	2.79	~591	90 ± 30	0.15	150 ± 40	0.25
$Ni/La_{1.5}Sr_{0.5}NiO_4/NiO_y$	2.32	~964	202 ± 4	0.21	300 ± 0	0.31
$Ni/LaSrNiO_4/NiO_y$	1.59	~707	65 ± 20	0.09	125 ± 22	0.18
$Ni/La_{1.5}Sr_{0.5}NiO_4/NiO_y$	2.9	–	113	–	181	
$Ni/La_{1.5}Sr_{0.5}NiO_4/NiO_y$	8.2	–	106	–	168	

the results of the impedance study wherein the charge-transfer resistance (R_3) value for methanol oxidation was highest on the latter electrode. On normalizing the electrode roughness as well as the mass of the dispersed Ni, however, the $Ni/La_2NiO_4/NiO_y$ electrode is found to be the most active, whereas the remaining modified complex oxide electrodes of the series have relatively low and more or less similar electrocatalytic activities (i.e., true current densities). For instance, at E = 0.60 V in 1 M KOH + 1 M CH_3OH at 25 °C, estimates of the true current density, j_t (=j_t/m, where m is the mass of Ni deposited on the oxide) are 0.21, 0.09, 0.13 and 0.11 mA cm^{-2} mg^{-1}. Thus, Sr substitution adversely affects the electrocatalytic activity of the dispersed Ni overlayer towards methanol oxidation.

To investigate the effect of the mass of dispersed Ni on the electrocatalytic activity of the electrode towards electro-oxidation of methanol, two more electrodes of $Ni/La_{1.5}Sr_{0.5}NiO_4$ containing higher amounts of dispersed nickel (2.9 and 8.2 mg cm^{-2}) were studied for electro-oxidation of methanol in 1 M KOH + 1M CH_3OH at 25 °C. The results, given in Table 3, show that the higher mass of the deposited Ni on the $Ni/La_{1.5}Sr_{0.5}NiO_4/NiO_y$ electrode is somewhat detrimental to the electrocatalysis of methanol oxidation.

A comparison of the apparent electrocatalytic activities of different similar complex oxide anodes in alkaline solution shows that the present electrodes modified by dispersed Ni are more active than other unmodified electrodes reported in literature [33–35,38]. For instance, Raghuveer et al. [34] observed j = 0.38, 1.47 and 1.87 mA cm^{-2} (at E = 0.6 V vs. Hg|HgO) on $La_{1.8}Sr_{0.2}CuO_4$, $La_{1.6}Sr_{0.4}CuO_4$ and $La_{1.9}Sr_{0.1}Cu_{0.9}Sb_{0.1}O_4$, respectively, in 3 M KOH + 2 M CH_3OH (25 °C). Raghuveer and Vishwanathan [33] have further examined the electrocatalytic activities of bulk and nanocrystalline $La_{1.8}Sr_{0.2}CuO_4$ in 1 M KOH + 1 M CH_3OH and found j = 1.83 and 4.90 mA cm^{-2} at E = 0.701 V (vs. Hg|HgO), respectively. Similar oxides ($La_{0.75}Sr_{0.25}CoO_{3-\delta}$) were investigated by Yu et al. [35] in 1 M KOH + 1 M CH_3OH for which j = 7.7–18.8 mA cm^{-2} at E = 0.701 V vs. Hg|HgO. However, recently Abdel Rahim et al. [44] found an enhanced current density for methanol oxidation on the graphite electrode modified by electro-deposited Ni, for which j was 63 mA cm^{-2} at E = 0.6 V vs. Hg|HgO (ν = 10 mV s^{-1}). On the other hand, glassy carbon modified by cobalt hydroxide produced only j = 1.67 mA cm^{-2} at E = 0.551 V (vs. Hg|HgO) in 1 M KOH + 0.5 M CH_3OH (ν = 50 mV s^{-1}) [3]. Thus, the electrocatalytic activities of all the above electrodes are reported to be low compared with those observed in the present study.

To investigate the influence of KOH and CH_3OH concentrations, E vs. log j curves for the $Ni/La_{1.5}Sr_{0.5}NiO_4/NiO_y$ electrode were determined for variation in KOH concentration while maintaining the methanol concentration (1.5 M) and the ionic strength of the medium (μ = 1.5) constant. The latter was achieved by using KNO_3 as an inert salt. To obtain the reaction order in OH^- concentration (p_{OH}), log j vs. log [KOH] curves at three constant potentials at 25 °C were constructed as shown in Fig. 11. All three plots are straight lines with approximately the same slope, i.e., the same order with respect to KOH concentration ($p_{OH} \approx 2$). By contrast, the effect of methanol concentration on the rate of reaction is complex, as shown in Fig. 12.

3.7. Mechanism

Considering the results of cyclic voltammetry, Tafel polarization and oxidation product analyses, we propose the following sequence of steps for methanol electro-oxidation on $La_{2-x}Sr_xNiO_4$ modified by dispersed Ni in KOH solutions:

$$Ni(III) + OH^- \leftrightarrow Ni(III)\cdot OH + e^- \quad (3)$$

$$Ni(III) + CH_3OH \leftrightarrow Ni(III)\cdot CH_3OH \quad (4)$$

$$Ni(III)\cdot CH_3OH + Ni(III)\cdot OH + OH^- \rightarrow Ni(III)\cdot CH_2O + Ni(III) + 2H_2O + e^- \quad (5)$$

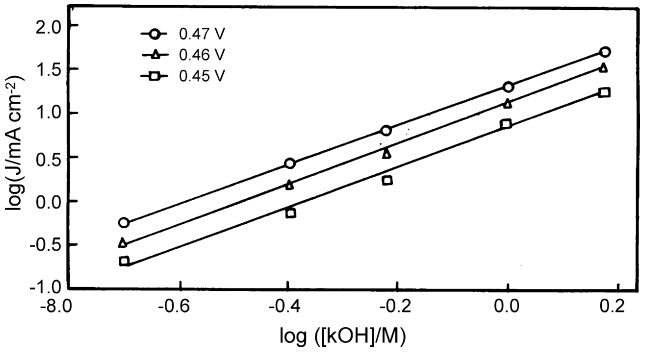

Fig. 11. Plot of log j vs. log [KOH] at constant potential for electro-oxidation of methanol at $Ni/La_{1.5}Sr_{0.5}NiO_4/NiO_y$ electrode in alkaline solutions (25 °C); E = 0.45 (□), 0.46 (Δ) and 0.47 (○) V; μ = 1.5 and [CH_3OH] = 1.5 M.

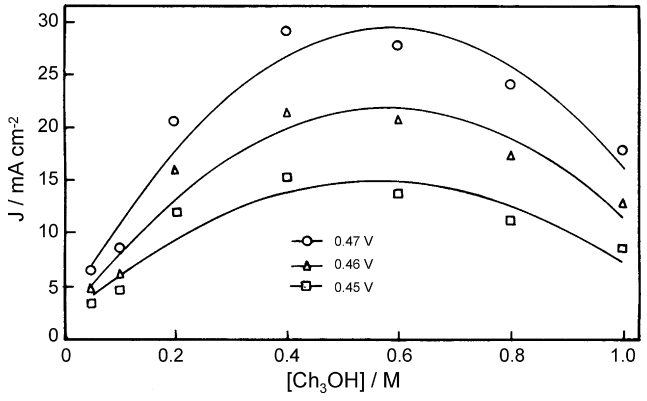

Fig. 12. Effect of methanol concentration on rate of methanol oxidation at $Ni/La_{1.5}Sr_{0.5}NiO_4/NiO_y$ electrode at three different potentials in 1 M KOH (25 °C).

$$\mathrm{Ni(III)\cdot CH_2O + Ni(III)\cdot OH + OH^- \underset{\text{fast}}{\longrightarrow} Product} \quad (6)$$

The involvement of OH and C—H—O species as intermediates in the electro-oxidation of methanol has been proposed in elsewhere ([9] and references therein). Taking reaction (5) as the rate-determining step (rds) and assuming that the total surface coverage is mainly by adsorbed OH and CH_3OH molecules (θ_T), the overall current density expression for methanol electro-oxidation can be written as:

$$j = nFk_5\theta_{OH}\theta_{CH_3OH}C_{OH^-}\exp\left(\frac{\beta FE}{RT}\right)$$

$$= \frac{nFk_5K_3K_4C_{CH_3OH}C_{OH^-}^2 e^{(1+\beta)FE/RT}}{(1+K_3C_{OH^-}e^{FE/RT}+K_4C_{CH_3OH})^2} \quad (7)$$

where θ_{OH} and θ_{CH_3OH} are the surface coverages by OH and CH_3OH molecules, respectively, and can be obtained by considering reactions (3) and (4) under quasi equilibrium conditions; K_3 and K_4 are the equilibrium constants for reactions (3) and (4), respectively; k_5 is the rate constant for the rate-determining step (5). All other symbols used in Eq. (7) have their usual meaning.

When OH and CH_3OH molecules are sparsely adsorbed on the electrode surface, Eq. (7) becomes:

$$j = nFk_5K_3K_4C_{OH^-}^2C_{CH_3OH}e^{(1+\beta)FE/RT} \quad (8)$$

Eq. (8) gives $\beta \cong 40\,\mathrm{mV\ decade^{-1}}$ assuming $\beta \approx 0.5$, where β is the symmetry coefficient for the anodic reaction and $p_{CH_3OH} = 1$ and $p_{OH} = 2$. Similar values of the observed Tafel slope and the order in OH^- concentration are also found for the reaction. When, however, the OH molecule is weakly adsorbed on the electrode surface, the rate equation becomes:

$$j = \frac{nFk_5K_3K_4C_{CH_3OH}C_{OH^-}^2 e^{(1+\beta)FE/RT}}{(1+K_4C_{CH_3OH})^2} \quad (9)$$

This equation explains fairly well the observed dependence of current density on methanol concentration (Fig. 12).

4. Conclusions

The study has demonstrated that the electrocatalytic activities of $La_{2-x}Sr_xNiO_4$ ($x = 0$, 0.25, 0.5 and 1) electrodes for methanol oxidation in alkaline solutions are greatly enhanced in the presence of Ni particles dispersed on their surfaces. Further, these modified electrodes do not suffer from poisoning by the intermediates/products of methanol oxidation. Among the oxide electrodes investigated, $La_{1.5}Sr_{0.5}NiO_4$ modified by dispersed Ni exhibits the best electrocatalytic activity. Adherence of the electrode materials to the Ni support is also very good.

Acknowledgements

This work was financially supported by the Department of Science and Technology (DST), Government of India, through a research project (SR/S1/PC-41). The authors also thank Prof. A.S.K. Sinha, Department of Chemical Engineering, and Prof. S.K. Sengupta, Department of Chemistry of Banaras Hindu University for measurement of the particle size of oxides and correction of the written Eglish, respectively.

References

[1] S. Wasmus, A. Kuver, Electrochim. Acta 45 (2000) 4319.
[2] X. Ren, P. Zelenay, S. Thomas, J. Davey, S. Gottesfeld, J. Power Sources 86 (2000) 111.
[3] M. Jafarian, M.G. Mahjani, H. Heli, F. Gobal, H. Khajehsharifi, M.H. Hamedi, Electrochim. Acta 48 (2003) 3423.
[4] G.T. Burstein, C.J. Barnett, A.R. Kucernak, K.R. Williams, Catalysis Today 38 (1997) 425.
[5] R. Parsons, T.J. Vandernoot, J. Electroanal. Chem. 257 (1988) 9.
[6] X. Ren, T.E. Springer, T.A. Zawodzmski, S. Gottesfeld, J. Electrochem. Soc. 147 (2000) 466.
[7] K. Scott, W.M. Taoma, P. Argyropoulas, K. Sundmacher, J. Power Sources 83 (1999) 2004.
[8] W. Li, J. Lu, J. Du, D. Lu, H. Chen, H. Li, Y. Wu, Electrochem. Commun. 7 (2005) 406.
[9] A.V. Tripkovic, K.D. Popovic, J.D. Momcilovic, D.M. Drazic, Electrochim. Acta 44 (1998) 1135.
[10] F. Seland, D.A. Harrington, R. Tunold, Electrochim. Acta 52 (2006) 773.
[11] J. Kua, W.A. Goddard, J. Am. Chem. Soc. 121 (1999) 10928.
[12] T. Iwasita, Electrochim. Acta 47 (2002) 3663.
[13] S. Tanaka, M. Umeda, H. Ojima, Y. Usui, O. Kimura, I. Uchida, J. Power Sources 152 (2005) 34.
[14] J. Jiang, A. Kucernak, J. Electroanal. Chem. 543 (2003) 187.
[15] J.B. Goodenough, A. Hammet, B.J. Kennedy, R. Manohara, S.A. Weeks, J. Electroanal. Chem. 240 (1988) 133.
[16] W. Sugimoto, T. Saida, Y. Takasu, Electrochem. Commun. 8 (2006) 411.
[17] C. Roth, N. Marty, F. Hahn, J.M. Liger, C. Lamy, H. Fuess, J. Electrochem. Soc. 149 (2002) E 433.
[18] K.-W. Park, K.-S. Ahn, Y.-C. Nah, J.-H. Choi, Y.-E. Sung, J. Phys. Chem. 107 (2003) 4352.
[19] P.C. Biswas, Y. Nodasaka, M. Enyo, J. Appl. Electrochem. 26 (1996) 30.
[20] J.W. Guo, T.S. Zhao, J. Prabhuram, C.W. Wong, Electrochim. Acta 50 (2005) 1973.
[21] J.W. Guo, T.S. Zhao, J. Prabhuram, R. Chel, C.W. Wong, Electrochim. Acta 50 (2005) 754.
[22] J. Prabhuram, T.S. Zhao, Z.X. Liang, R. Chen, Electrochim. Acta 52 (2007) 2649.
[23] D. Pan, J. Chen, W. Tao, L. Nie, S. Yao, Langmuir 22 (2006) 5872.
[24] G.-Y. Zhao, C.-L. Xu, D.-J. Guo, H. Li, H.-L. Li, J. Power Sources 162 (2006) 492.
[25] V. Neburchilov, H. Wang, J. Zhang, Electrochem. Commun. 9 (2007) 1788.
[26] F.S. Hoor, C.N. Tharamani, M.F. Ahmed, S.M. Mayanna, J. Power Sources 167 (2007) 18.
[27] E. Antolini, J. Power Sources 170 (2007) 1.
[28] H.J. Salavagione, C. Sanchis, E. Morallon, J. Phys. Chem. C 111 (2007) 12454.
[29] J.J. Wang, G.P. Yin, J. Zhang, Z.B. Wang, Y.Z. Gao, Electochim. Acta 52 (2007) 7042.
[30] K. Lasch, G. Hayn, L. Jorissen, J. Garche, O. Besenhardt, J. Power Sources 105 (2002) 305.
[31] T. Ohmore, K. Nodasaka, M. Enyo, J. Electroanal. Chem. 281 (1990) 331.
[32] P.C. Biswas, M. Enyo, J. Electroanal. Chem. 322 (1992) 203.
[33] V. Raghuveer, B. Viswanathan, Fuel 81 (2002) 2191.
[34] V. Raghuveer, K.R. Thampi, N. Xanthopoulos, H.J. Mathieu, B. Viswanathan, Solid State Ionics 140 (2001) 263.
[35] H.-C. Yu, K.-Z. Fung, T.-C. Guo, W.-L. Chang, Electrochim. Acta 50 (2004) 811.
[36] K. Deshpande, A.S. Mukasyan, A. Varma, J. Power Sources 158 (2006) 60.
[37] A. Lan, A.S. Mukasyan, J. Phys. Chem. C 111 (2007) 9573.
[38] R.N. Singh, T. Sharma, A. Singh, Anindita, D. Mishra, S.K. Tiwari, Electrochim. Acta 53 (2008) 2322.
[39] J.K. Vassiliou, M. Hombostel, R. Ziebarth, F.J. Disalvo, J. Solid State Chem. 81 (1989) 208.
[40] R.N. Singh, T. Sharma, A. Singh, J. New Mater. Electrochem. Syst. 10 (2007) 105.
[41] R.N. Singh, J.-F. Koenig, G. Poillerat, P. Chartier, J. Electrochem. Soc. 137 (1990) 1408.
[42] R.N. Singh, J.P. Pandey, K.L. Anitha, Int. J. Hydrogen Energy 18 (1993) 467.
[43] A. Seghiouer, J. Chevalet, A. Barhoun, F. Lentelme, J. Elerctroanal. Chem. 442 (1998) 113.
[44] M.A. Abdel Rahim, R.M. Abdel Hameed, M.W. Khalil, J. Power Sources 134 (2004) 160.
[45] Y.-C. Liu, X.-P. Qiu, W.-T. Zhu, G.-S. Wu, J. Power Sources 114 (2003) 10.
[46] J.T. Mueller, P.M. Urban, J. Power Sources 75 (1998) 139.
[47] Y. Bultel, L. Genies, O. Antoine, P. Ozil, R. Durand, J. Electroanal. Chem. 527 (2002) 143.
[48] L.A. da Silva, V.A. Alves, M.A.P. da Silva, S. Trasatti, J.F.C. Boodts, Electrochim. Acta 42 (1997) 271.
[49] R.N. Singh, S.K. Tiwari, S.P. Singh, N.K. Singh, G. Poillerat, P. Chartier, J. Chem. Soc. Faraday Trans. 92 (1996) 2593.
[50] S. Trasatti, in: J. Lipkowasky, P.N. Ross (Eds.), The Electrochemistry of Novel Materials, VCH, Weinheim, 1994, p. 207.
[51] N. Priyantha, P. Jayaweera, D.D. Macdonald, A. Sun, J. Electroanal. Chem. 572 (2004) 409.
[52] B.D. Cahan, M.L. Daroux, E.B. Yeager, J. Electrochem. Soc. 136 (1989) 1585.